Nonlocal transport in toroidal plasma devices in the presence of magnetic perturbations

G. Spizzo[1], R.B. White[2], M. Maraschek[3], V. Igochine[3], G. Granucci[4],
the ASDEX Upgrade Team[3] and the EUROfusion MST1 Team *
[1] *Consorzio RFX, Padova, Italy*
[2] *Plasma Physics Laboratory, Princeton, NJ (USA)*
[3] *Max-Planck-Institut for Plasmaphysics, Garching, Germany*
[4] *IFP-CNR, Milano, Italy*
* *see the author list of B. Labit et al., 2019 Nucl. Fusion accepted*

Collisional particle transport in the presence of field perturbations originating from various MHD activity is examined theoretically on tokamaks (ITER, ASDEX Upgrade (AUG), NSTX and DIII-D) and the reversed-field pinch RFX-mod [1]. For ITER and AUG, modes typically leading to a disruption [2] are considered. On NSTX and DIII-D unstable Alfvén modes are investigated. Finally on the RFX-mod the effect of saturated tearing modes is studied. It is well known that transport is not always diffusive in situations involving stochastic magnetic fields [3]. These publications consider a *model stochastic field*, and evaluate the transport in terms of correlation times and lengths (parallel $L_\parallel$ and perpendicular $L_\perp$), related to the Kubo number K, and the Kolmogorov length L_k, and particle orbit properties such as the mean square displacements $\langle \mathrm{d}x^2 \rangle$:

$$K = \frac{\delta B}{B}\frac{L_\parallel}{L_\perp}, \quad \langle \mathrm{d}x^2 \rangle \sim e^{L_k t} \tag{1}$$

For $0.3 < K < 1$, it is shown that the diffusion coefficient D follows the quasilinear scaling $D \approx K^2 L_\perp^2 / L_\parallel$. The extension of this theory to typical experimental situations with a *real stochastic field* in a fusion device is not straightforward: what are the K, L_k numbers in a typical discharge? Often the perturbation spectrum is very sparse, not leading to well-defined mean values for these parameters: the evaluation made in RFX with the assumption $L_\perp \sim a$ shows that $K \approx 1.5$ for a typical tearing mode spectrum, but can vary in between this value and $K \sim 10$, depending on perturbation strength [4]. Moreover, the calculation of $L_\parallel$ in Eq. (1) is questionable in a finite-size device.

ITER. We consider an advanced scenario equilibrium for ITER [5]. We use the guiding-center code ORBIT [6] to analyze test particle (electron and ion) transport in presence of the full 3D magnetic field (equilibrium plus perturbations). Perturbations are described through the representation $\delta\vec{B} = \nabla \times \alpha(\psi_p)\vec{B}$, and Boozer co-ordinates (ψ_p, θ, ζ) are used [6]. A kinetic Poincaré plot is used to show the nature of the particle trajectories: these are plots of 1 keV passing (magnetic moment $\mu = 0$) deuterium trajectories, to show the effect of the field on the particles. Modes used are $\omega = 0$ global, tearing modes corresponding to a pre-disruptive phase with the largest mode being $\alpha_{2,1} = 2 \times 10^{-3}A$: A is a scaling factor, $0 < A < 1$, where $A = 1$ is the “natural” amplitude for the case considered. Fig. 1 shows these plots for $A = 0.3$ and $A = 1$. For $A = 0.3$ many Kolmogorov-Arnold Moser (KAM) surfaces [7] are intact, with the dominant resonances $m/n = 3/2$ and $2/1$ clearly visible, but also the $5/3$ arising from the interaction of the main resonances. There are of course many higher order Fibonacci sequence islands. The case with $A = 1$ is more chaotic, and one could expect that non-diffusive, “anomalous” transport should be present only with these high perturbation amplitudes. This is wrong, since resonances can produce long time correlations and dynamical traps [7] for particle trajectories at perturbation amplitudes *much too small* for the orbits to be represented as uniformly chaotic. To examine this point, we launch particles near the mid-radius ($\psi_p = 0.6$), uniform pitch $v_{\parallel}/v$, and follow them for many collision times. Since we are interested in the asymptotic nature of transport, we fit the time series $(P_\zeta(t) - P_\zeta(0))^2$ to Dt^p using only late times, least-square fitting the curve and finding the best values of diffusivity D and exponent p. Plots of D, p versus A are shown in Fig. 2: for very small mode amplitudes, collisional diffusion is only slightly augmented by perturbations, and transport is overall diffusive ($p = 1$). Subdiffusion [8] with $p = 0.5$ begins for surprisingly small amplitudes, $A = 0.3$ for 1 keV ions with collision frequency $\nu T = 10^{-2}$ (T is the ion toroidal transit time). It is worth underlining that $A = 0.3$ corresponds to the rather conserved Poincaré plot of Fig. 1(left). Collisions tend to cut long range, Lévy flights, and when $\nu T = 0.1$ (ten toroidal turns) transport is not as strongly modified. The same effect is obtained by increasing ion energy to $E = 10$ keV (squares). In the case of electrons with $E = 10$ keV and $\nu T = 10^{-1}$, a similar analysis shows instead that subdiffusion is found to occur at very low mode amplitude, $A \sim 0.15$. At these small amplitudes, most of the domain covered by particles consists of good KAM surfaces, but of course there are very small resonances, not visible in a large-scale Poincaré plot such that of Fig. 1, still

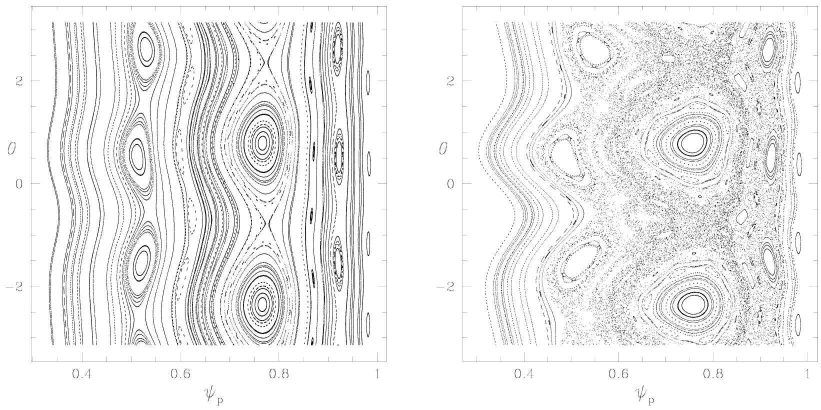

Figure 1: *ITER: Kinetic Poincaré plots, with amplitudes* $A = 0.3$ *(left) and natural amplitude* $A = 1$ *(right), shown vs the normalized poloidal flux* ψ_p.

influencing electron orbits.

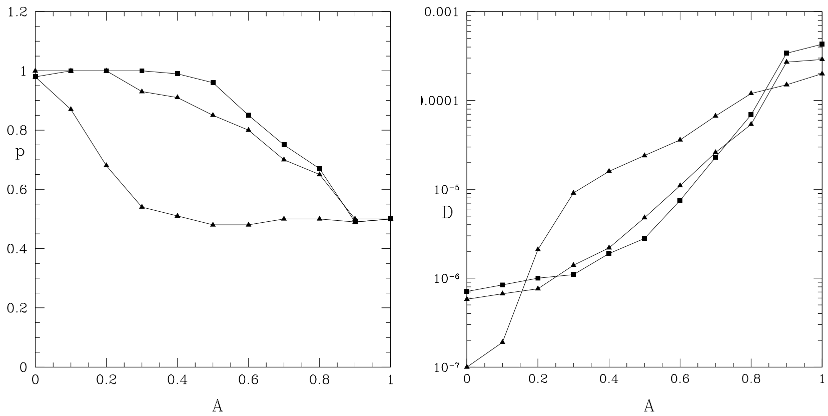

Figure 2: *ITER: Plots of p (left) and D (right) vs A. Triangles for p are for 1 keV ions with* $\nu T = 10^{-2}$ *(lowest curve) and* 10^{-1} *(upper curve), and squares are for 10 keV ions with* $\nu T = 10^{-2}$. *D is in* ORBIT *units (gyroradius* ρ *and transit time* T*).*

NSTX and DIII-D. In the case of NSTX, a spectrum of TAE modes has been observed and analyzed using NOVA [9]. The frequency of the modes is $\omega \sim$ 100 kHz, largest $\alpha_{2,5} = 6.5 \times 10^{-7}$. Ion velocity is too small to explore the field structure in one mode period, and ion transport was found to be diffusive for all amplitude values. On the contrary, electron transport ($E = 2$ keV and $\nu T = .0025$) is diffusive ($p = 1$) up to $A \sim 0.8$, and then rapidly falls down to strong subdiffusion, with $p = 0.4$, dropping to $p = 0.16$ for $A > 1.5$ and complete stochastic loss. In the case of DIII-D, saturated TAE mode amplitudes are derived by scaling the prediction of a synthetic ECE diagnostic applied to NOVA calculated eigenfunctions. DIII-D has a wider spectrum of modes than does NSTX: there are 8 different modes with $1 \leq n \leq 5$ and a total of 105 poloidal harmonics, largest eigenfunction $\alpha \sim 6 \times 10^{-7}$ and frequency $62 < \omega < 80$ kHz. In this case the mode spectrum is broad enough to produce diffusion of ions and electrons with energy $E = 1$ keV and $\nu T = 10^{-2}$ for all mode amplitudes A, no transition to subdiffusion with $p < 1$. The spectrum is such to make the random-phase approximation valid, and to preclude strong subdiffusion.

AUG. A further example of pre-disruption scenario has been considered in AUG [2], i.e. the L-mode, high density shot # 30984, at t=1.398 seconds. Main modes are $\alpha_{2,1} = 1.3 \times 10^{-4}$, $\alpha_{3,1} = 1.5 \times 10^{-4}$, $\alpha_{4,1} = 8.9 \times 10^{-5}$ and $\alpha_{5,1} = 5 \times 10^{-5}$, frequency $\omega = 1.7$ kHz. In the AUG case, the α profiles are the "Meskat" eigenfunctions [10], fitted to experimentally measured $\dot{B}_\theta$. Clear resonance islands are seen for each harmonic, as well as a nonlinearly generated resonance at $m/n = 5/2$ (Fig. 3). We chose three different initial surfaces (red lines in Fig. 3). Thermal electrons with $E = 300$ eV and $\nu T = 10^{-2}$, launched at $\sqrt{\psi} = 0.4$, are within the orbits rotating around the $2/1$ resonance, and transport is superdiffusive with $p = 1.23$. Electrons launched at $\sqrt{\psi} = 0.6$ are near the $5/2$ resonance, and transport is strongly subdiffusive, with $p = 0.2$, while the stochastic domain at $\sqrt{\psi} = 0.8$ is also subdiffusive with $p = 0.5$, and a much larger D

than in the case at $\sqrt{\psi} = 0.6$. It is striking that the large $m = 2$ island, with no apparent stochasticity, nevertheless produces much stronger electron transport than does the stochastic domain, confirming the traditional picture that this island has a fundamental role in the thermal quench preceding disruption [10]. **RFX-mod.** The chaotic state of the reversed-field pinch RFX-mod has a broad spectrum of stationary ($\omega = 0$) saturated tearing modes with $m = 0, 1$ and $n \leq 24$, with largest mode $\alpha_{1,10} = 7.7 \times 10^{-4}$. Both thermal ions and electrons ($E = 250$ eV and $\nu T = 0.4$) are found to be subdiffusive, with $p = 0.6$. As a consequence, in RFX the use of a traditional diffusive-convective scheme for transport, which is expressed by the Fick's law $\vec{\Gamma} = -D\vec{\nabla}n + \vec{v}n$, with D estimated from the Rechester-Rosenbluth formula and leading to the well known transport scalings, is questionable. In RFX a nonlocal model of transport, based on the Montroll formalism and similar in principle to fractional transport [11] has been developed, quantitatively reproducing experimental results [4].

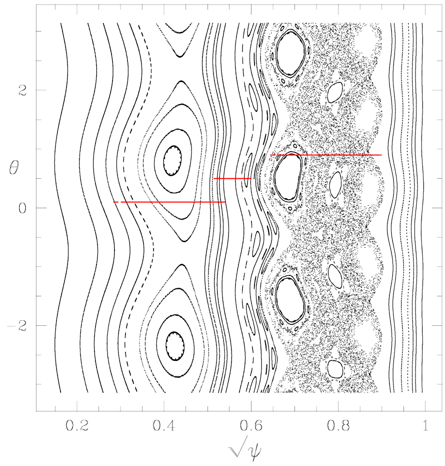

Figure 3: *AUG: Poincaré plot made with co-passing ($v_\parallel/v = 1$) collisionless electron orbits. Red horizontal lines mark the location of the particles launched for the determination of p.*

This work has been carried out within the framework of the EUROfusion Consortium and has received funding from the Euratom research and training programme 2014-2018 and 2019-2020 under grant agreement No 633053. The views and opinions expressed herein do not necessarily reflect those of the European Commission.

References

[1] G. Spizzo *et al*, Nucl. Fusion **59**, 016019 (2019)

[2] M. Maraschek *et al*, Plasma Phys. Controlled Fusion **60**, 014047 (2018)

[3] M. B. Isichenko, Plasma Phys. Controlled Fusion **33**, 795 (1991); F. Spineanu, M. Vlad and J. Misguich, J. Plasma Phys. **51**, 113 (1994); M. Vlad, F. Spineanu, J. Misguich and R. Balescu, Physical Review E **67**, 026406 (2003); R. Balescu, H.D. Wang and J. Misguich, Phys. Plasmas **1**, 3826 (1994)

[4] G Spizzo, R B White, S Cappello, and L Marrelli, Plasma Phys. Controlled Fusion **51**, 124026 (2009)

[5] Y. Gribov, `ftp://pfctrl@ftp.jp.iter.org/array1/PFcontrol/EQDSKfiles/Code PET/Scenario 4beta scanPET/`

[6] R. B. White and M. S. Chance, Phys. Fluids **27**, 2455 (1984)

[7] G.M. Zaslavsky, Hamiltonian Chaos and Fractional Dynamics (Oxford University Press) p. 187–199 (2005)

[8] R. Sanchez and D.E. Newman, Plasma Phys. Controlled Fusion **57**, 123002 (2015)

[9] R. B. White, N. Gorelenkov *et al*, Plasma Phys. Controlled Fusion **58**, 115007 (2016)

[10] V. Igochine, *et al.*, Plasma Phys. Control. Fusion **43**, 1325 (2001)

[11] D. del Castillo-Negrete, AIP Conf. Proc. **1013**, 207 (2008)